COB-2021-0297
A robust strategy to stabilize aircraft landing gear shimmy under structural uncertainties

Luis Eduardo Prado Pereira
luiseduardopp@usp.br
José Augusto Ignácio da Silva
j.i.silva@usp.br
Flávio Donizeti Marques
fmarques@sc.usp.br

Deapartment of Mechanical Engineering
São Carlos School of Engineering
University of São Paulo
Av. Trabalhador São-carlense, 400, 13566-590, São Carlos, SP, Brazil

Abstract. *Shimmy in aircraft landing gears is a dynamic instability commonly caused by structural and tyre-to-ground interaction. The instability onset conditions can be predicted with linearized models that depend primarily on the structural dynamics and simplified linear tyre loads. The shimmy self-excited mechanism is driven by divergent unstable motion that can define the phenomenon's boundaries in terms of vertical force and forward speed, limiting the aircraft's operational landing envelope. The control of the shimmy instability has been performed with passive and active techniques. Although there are different control design strategies, the shimmy dynamics' stabilization is still a formidable challenge. In this context, this work proposes an approach to suppress unstable shimmy motion, considering uncertainties on a landing gear structure. The landing gear model comprises torsional landing gear dynamics and tyre loads based on nonlinear coupled lateral displacement and self-alignment angular motion. Polytopic convex hulls are used to describe the uncertainties, and Lyapunov's stability function with Linear Matrix Inequalities (LMIs) are used to design a robust controller. Numerical simulations are carried out to demonstrate that the control gain can asymptotically stabilize the system responses to assure a safe shimmy-free landing envelope. A complete analysis of the control performance is also presented.*

Keywords: *Shimmy, Aircraft landing gears, Structural uncertainties, Robust controller, LMIs*

1. INTRODUCTION

Shimmy is an aeromechanical phenomenon that occurs in the aircraft's landing gears (LG) when it is contact with the ground. This phenomenon is associated with a self-excitation state of oscillations caused by the dynamic interaction of the tyre-to-ground (Somieski, 1997). The shimmy occurrence results in a potential of instability that can introduce high levels of vibrations in the LG's structure, which can cause fatigue and structural limb failures. For this reason, the shimmy phenomenon is undesirable and the study of techniques to suppress or alleviate it becomes very important for the aerospace industry.

The dynamic characterization of shimmy in LG's structures is described by the works (Somieski, 1997; Esmailzadeh and Farzaneh, 1999; Thota *et al.*, 2010; Rahmani and Behdinan, 2019a). Passive solutions to control this type of instability has been also reported in the works (Li *et al.*, 2017; Rahmani and Behdinan, 2019c,b; Laporte *et al.*, 2020). Despite the authors discuss that passive dampers can mitigate shimmy vibrations, their performance can substantially reduce when operating in different conditions related to those for which they are previously designed. On the other hand, using active control strategies is an attractive option to suppress this phenomenon because they allow one to develop adaptive controllers simpler.

In this context, Tourajizadeh and Zare (2016) compared a optimal control strategy with sliding mode controller to stabilize the shimmy in the presence of uncertainty and external disturbances. Orlando and Alaimo (2017) designed a robust non-linear controller to suppress the torsional shimmy with torque link free-play. Recently, Orlando (2020) applied adaptive control techniques to suppress the shimmy in the landing gear.

In particular, for this study, robust controllers are designed to suppress the shimmy vibrations considering structural uncertainties. A benchmark model to characterize this linear phenomenon is used, and the control action is achieved by using a classical electro-mechanical actuator. Parametric uncertainties are considered in LG's stiffness and damping, described in terms of convex polytopic hulls to design the active controllers. A complete state feedback scheme is used and the controllers gains are determined based on the Lyapunov's theory applied to the linear quadratic regulator (LQR) problem with decay rate (γ) restriction solved by means linear matrices inequalities (LMIs), following the Refs. (Olalla *et al.*, 2009; da Silva *et al.*, 2019). The results demonstrate that this proposed LMI-based controller can be used to suppress shimmy instabilities, asymptotically stabilizing the aircraft landing operational envelope under presence of model's uncertainties.

2. TORSIONAL SHIMMY MATHEMATICAL MODEL

The benchmark model to study torsional shimmy in this work was based on (Somieski, 1997; Thota *et al.*, 2010; Tourajizadeh and Zare, 2016; Orlando and Alaimo, 2017; Orlando, 2020). As in real applications, here the inputs that represent the torsional shimmy are: the vertical force applied on the structure (F_z) and the airplane forward velocity (V). According with appropriate combination of these parameters, the torsional shimmy is observed. The mechanical model used in this work consists of a turning tube and a sliding tube that are connected by a collar. The Figure 1 is a sketch of the assembly, which shows the structure parts. The torque link assure that the turning and the sliding tubes can move freely in the vertical direction. The landing gear structure are linked to a wheel by a caster with length e. Only the torsional motion ($\psi(t)$), it is make possible to the system. The mass inertia moment of the assembly is I_z about the z-axis and the nominal stiffness and damping of the structure induced by torsional suspension of the LG are accounted for by k_ψ and c_ψ. The tyre-ground interaction moment applied to the LG structure is accounted by $M_{T_\psi}(\lambda, \dot{\psi})$. In addition, the control moment applied by the electro-mechanical actuator is represented by $M_c(t)$.

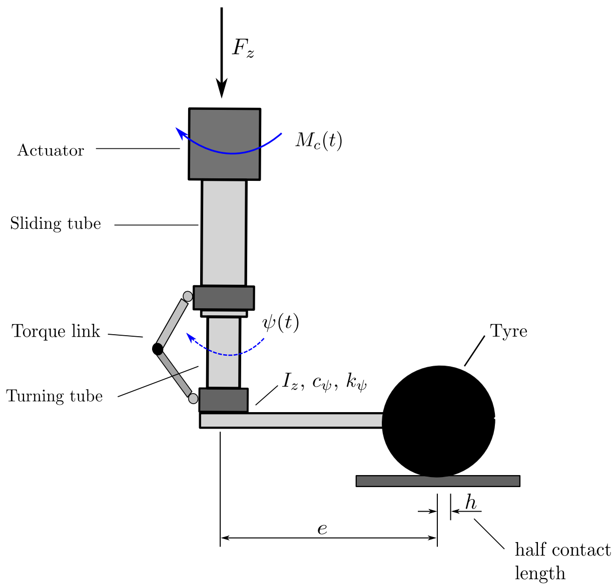

Figure 1. Sketch of the torsional shimmy model.

The differential equation of the motion that represents the shimmy dynamic can described by (Somieski, 1997):

$$I_z\ddot{\psi}(t) + c_\psi\dot{\psi}(t) + k_\psi\psi(t) + M_{T_\psi}(\dot{\psi}, \lambda) = M_c(t) \tag{1}$$

The tyre-ground interaction moment $M_{T_\psi}(\lambda, \dot{\psi}) = M_{K_\alpha} + eF_{K_\lambda}(\lambda) + M_{D_\lambda}(\dot{\psi})$, comprises the moment due to the restoring force of the tyre ($F_{K_\lambda}(\lambda)$), the self-aligning moment ($M_{K_\alpha}(\lambda)$) and the tyre's tread damping moment ($M_{D_\lambda}(\dot{\psi})$), with λ being the lateral deformation of the main contact point between the tyre and the ground. Following a linear approach of these efforts, the following relationships must be hold (Somieski, 1997; Thota *et al.*, 2010):

$$\begin{aligned} M_{K_\alpha} &= \frac{k_\alpha F_z}{L}\lambda \\ F_{K_\lambda} &= \frac{7k_\lambda F_z}{L}\lambda \\ M_{D_\lambda}(\dot{\psi}) &= \frac{c_\lambda}{V}\dot{\psi} \end{aligned} \tag{2}$$

where k_α and k_λ are the torsional and lateral stiffness of the tyre, respectively, c_λ represents the lateral damping of the tyre.

The control moment $M_c(t)$ is achieved by introducing an electro-mechanical actuator. It is proportional to the control input signal $u(t)$ (i.e., voltage applied in the actuator) with the moment constant k_e, as the following:

$$M_c(t) = k_e u(t) \quad . \tag{3}$$

The tyre's lateral dynamic is modeled by Von Schlippe theory, as the following (Somieski, 1997):

$$\dot{\lambda}(t) + \frac{V}{L}\lambda(t) = V\psi(t) + (e-h)\dot{\psi}(t) \tag{4}$$

where h is the half contact patch length of the tyre with the ground and L is the relaxation length that commonly exhibit the values $L \approx 3h$.

Combining Eqs. (1), (2), (3) and (4), the following dynamic model is obtained

$$\begin{cases} I_z\ddot{\psi}(t) + \left(c_\psi + \frac{c_\lambda}{V}\right)\dot{\psi}(t) + k_\psi\psi(t) + \frac{F_z}{L}\left(k_\alpha + 7ek_\lambda\right)\lambda(t) = k_e u(t) \\ \dot{\lambda}(t) + \frac{V}{L}\lambda(t) = V\psi(t) + (e-h)\dot{\psi}(t) \end{cases} \tag{5}$$

and its representation using the state space realization of Eq. (5) results in,

$$\dot{\mathbf{x}}(t) = \mathbf{A}\mathbf{x}(t) + \mathbf{B}u(t) \tag{6}$$

where $\mathbf{x}(t) = \begin{bmatrix}\psi(t) & \dot{\psi}(t) & \lambda(t)\end{bmatrix}^T$ is the state vector. The matrices $\mathbf{A} \in \mathbb{R}^{n\times n}$ and $\mathbf{B} \in \mathbb{R}^{n\times m}$ are respectively, the dynamic and control input matrices, with n and m representing the number of states and control inputs, respectively. These matrices are given by,

$$\mathbf{A} = \begin{bmatrix} 0 & 1 & 0 \\ -\frac{k_\psi}{I_z} & -\left(\frac{c_\psi}{I_z} + \frac{c_\lambda}{I_z V}\right) & -\frac{F_z}{I_z L}\left(k_\alpha + 7ek_\lambda\right) \\ V & (e-h) & -\frac{V}{L} \end{bmatrix}, \qquad \mathbf{B} = \begin{bmatrix} 0 \\ k_e \\ 0 \end{bmatrix} \tag{7}$$

2.1 Structural Uncertainties Modeling

Parametric uncertainties are considered in LG's structural stiffness (k_ψ) and damping (c_ψ), by introducing the parameter δ that accounts the uncertainty fluctuation around the nominal value of the parameter, which results in:

$$\begin{cases} k_\psi = k_{\psi_0} + \delta k_{\psi_0} \\ c_\psi = c_{\psi_0} + \delta c_{\psi_0} \end{cases} \quad . \tag{8}$$

where c_{ψ_0} and k_{ψ_0} are the nominal LG's structural damping and stiffness. The parameter δ can vary by the range $-\delta_0 \leq \delta \leq \delta_0$, with δ_0 being the uncertainty level considered in the controller's design. It is very easy to note that these uncertain structural parameters are bounded by minumum and maximum values, i.e., $c_\psi = [c_{\psi_{min}}, c_{\psi_{max}}]$ and $k_\psi = [k_{\psi_{min}}, k_{\psi_{max}}]$, that depends directly of δ_0 intensity.

In order to perform the control design, a convex polytopic hull is used to represent the system under these uncertainties. Once, only the dynamic matrix $\mathbf{A}$ contains these parameters, the control matrix $\mathbf{B}$ is always constant in this analysis. Therefore, the uncertain plant can be represented by:

$$\dot{\mathbf{x}}(t) = \left(\sum_i^4 \alpha_i \mathbf{A}_i\right)\mathbf{x}(t) + \mathbf{B}u(t), \qquad \sum_{i=1}^4 \alpha_i = 1 \tag{9}$$

where α_i is used to describe the simplex unitary hull and $\mathbf{A}_i$, $i = 1,\ldots,4$, are the sub-systems obtained by combination of minimum and maximum values of c_ψ and k_ψ (i.e., vertices of the polytopic system). In particular to this work, two uncertain parameters are used, which leads to a four sub-systems, that can be calculated as $\mathbf{A}_1 = \mathbf{A}(c_{\psi_{min}}, k_{\psi_{min}})$, $\mathbf{A}_2 = \mathbf{A}(c_{\psi_{min}}, k_{\psi_{max}})$, $\mathbf{A}_3 = \mathbf{A}(c_{\psi_{max}}, k_{\psi_{min}})$ and $\mathbf{A}_4 = \mathbf{A}(c_{\psi_{max}}, k_{\psi_{max}})$, with $\mathbf{A}(c_\psi, k_\psi)$ representing the application of matrix $\mathbf{A}$ (cf. Eq. (7)) at particular values of c_ψ and k_ψ. Based on this modeling, the uncertain design space can be represented by a rectangle (cf. Figure 2), and the controllers must be designed to assure the system's stability for its whole area.

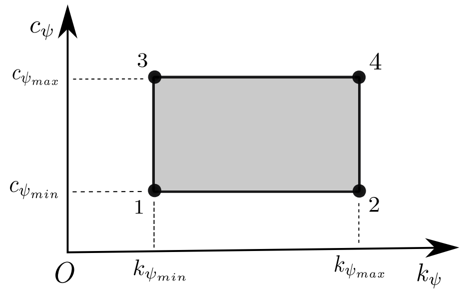

Figure 2. Illustration of the convex polytopic domain for controllers design.

3. ON THE ROBUST CONTROLLER'S DESIGN

A full state feedback controller gain is used to mitigate the shimmy phenomenon and stabilize the landing gear. The control method is based on those proposed in references (Olalla *et al.*, 2009), which consists of solving a linear convex optimization problem in terms of LMIs. The method is based on the Lyapunov stability theory and results in a simple structure's final state feedback gain.

Considering the controlled uncertain shimmy plant represented by Eq. (9), the strategy is to determine a state feedback control gain, $\mathbf{K}$, by the control law $\mathbf{u}(t) = \mathbf{K}\mathbf{x}(t)$, such that the following closed loop system is asymptotically stabilized.

$$\dot{\mathbf{x}}(t) = (\mathbf{A}(\alpha) + \mathbf{B}\mathbf{K})\mathbf{x}(t) \ , \tag{10}$$

where α indicates the presence of the uncertainties.

The linear quadratic regulator problem is used in this work to design the the controller gains in terms of LMIs. A sufficient condition to ensure the asymptotic stability of the system and minimize the LQR performance index, $J = \int_0^\infty (\mathbf{x}^T\mathbf{Q}\mathbf{x} + \mathbf{u}^T\mathbf{R}\mathbf{u})\, dt$ (Olalla *et al.*, 2009), in terms of LMIs is used in this work and given by the Theorem 1. The matrices $\mathbf{Q}$ and $\mathbf{R}$ are used to balance the transient performance and energy demand of the controllers.

Theorem 1 *A state-feedback gain* $\mathbf{K}$ *that stabilizes asymptotically the system from Eq.* (10) *and guaranteed cost* J *and decay rate* γ*, if there are matrices* $\mathbf{W} = \mathbf{W}^T \in \mathbb{R}^{n\times n}$, $\mathbf{Z} \in \mathbb{R}^{m\times n}$, $\mathbf{X} \in \mathbb{R}^{n\times n}$*, such that they satisfy the following LMIs:*

$$\begin{aligned} &\textit{min} \quad Tr(\mathbf{QW}) + Tr(\mathbf{X}) \\ &\qquad \textit{subject to} \\ &\mathbf{A}_i\mathbf{W} + \mathbf{BZ} + \mathbf{WA}_i^T + \mathbf{Z}^T\mathbf{B}^T + 2\gamma\mathbf{W} < \mathbf{0}, \quad i = 1, \dots, 4 \\ &\begin{bmatrix} \mathbf{X} & \mathbf{R}^{1/2}\mathbf{Z} \\ \mathbf{Z}^T\mathbf{R}^{1/2} & \mathbf{W} \end{bmatrix} > \mathbf{0}, \quad \mathbf{W} > \mathbf{0} \end{aligned} \tag{11}$$

where the Lyapunov matrix and the state feedback gain are respectively given by $\mathbf{P} = \mathbf{W}^{-1}$ *and* $\mathbf{K} = \mathbf{W}^{-1}\mathbf{Z}$*.*

Proof: See da Silva *et al.* (2019).

4. RESULTS AND DISCUSSIONS

To illustrate the presented approach numerical simulations are carried out considering the LG's parameters defined in Thota *et al.* (2010), for which the system's physical and geometric properties are shown in Table 1. The shimmy stability analysis is performed to find the instabilities boundaries (i.e., range of forward speeds where the phenomenon takes place) and the robust control design is done by using the introduced formulation.

4.1 Linear Shimmy Analysis

Figure 3 depicts the evolution of real part of eigenvalues of the dynamic matrix with the forward velocity V, for the torsional shimmy model, considering the vertical force (F_z) as 150 kN. The linear shimmy phenomenon is identified when the real part of the eigenvalues of the dynamic matrix reaches zero (i.e., $\mathcal{R}e(\rho_i) = 0$, where ρ_i referring to the eigenvalues of the state matrix $\mathbf{A}$, with $i = 1, \dots, 3$). It is observed that for this vertical force level, the linear shimmy boundary is defined in following range of forward velocity, $V = [4,\ 134.75]$ m/s. It is also verified that the more critical instability condition occurs at $V = 19.5$ m/s, highlighted by highest positive value of real part of eigenvalues. Additionally, Figure 4 shows the time histories of the structure for different levels of forward velocity inside the shimmy boundary of instability.

In order to verify the effect of structural uncertainties in the dynamic behavior of system, robust shimmy boundaries were built considering two uncertain levels (i.e., $\delta_0 = 10\%$ and $\delta_0 = 20\%$). An eigenvalue analysis of the four sub-systems

Table 1. Parameters of the shimmy model.

Parameter	**Value**
Caster length (e)	0.12 m
Torsional stiffness of the structure (k_ψ)	$3.8 \cdot 10^5$ N m rad^{-1}
Torsional damping of the structure (c_ψ)	300 N m s rad^{-1}
Mass inertia moment on the z-axis (I_z)	100 kg m^2
Half contact patch length (h)	0.1 m
Damping coefficient of the tyre (c_λ)	570 N m^2 rad^{-1}
Torsional stiffness of the tyre (k_α)	1 m rad^{-1}
Lateral stiffness of the tyre (k_λ)	0.002 rad^{-1}
Relaxation length (L)	0.3 m
Vertical force (F_z)	150 kN
Actuator Moment (k_e)	1000 N m

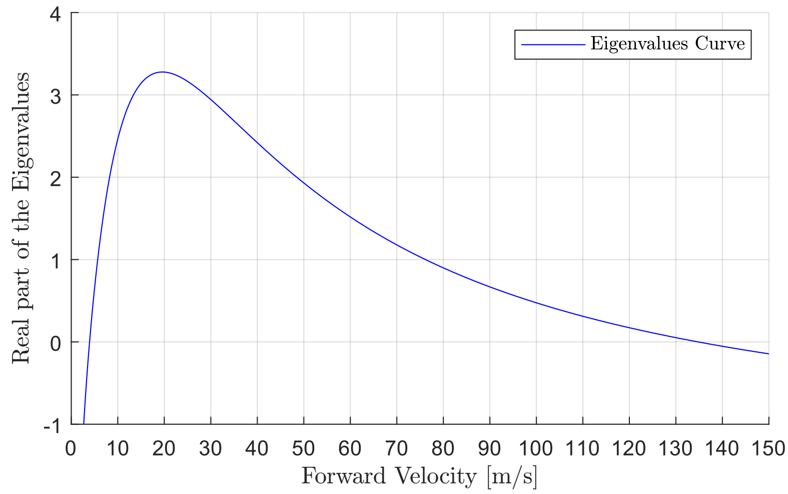

Figure 3. Linear shimmy boundary.

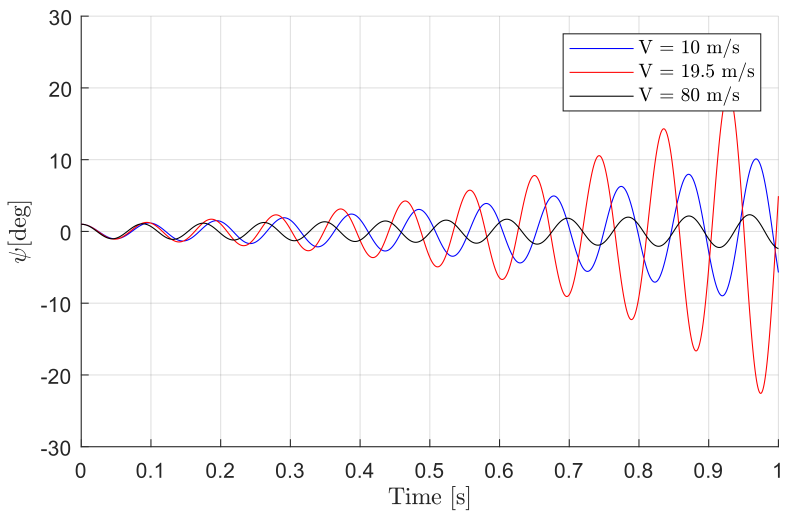

Figure 4. Time histories of system in shimmy instability.

(i.e., vertices of the polytopic system) is shown in Figure 5(a,b), respectively, for each considered level of uncertainty. Based on these results, it is observed more critical instabilities when the LG's stiffness and damping are minimum (i.e., vertex 1 of the polytope), which is physically expected.

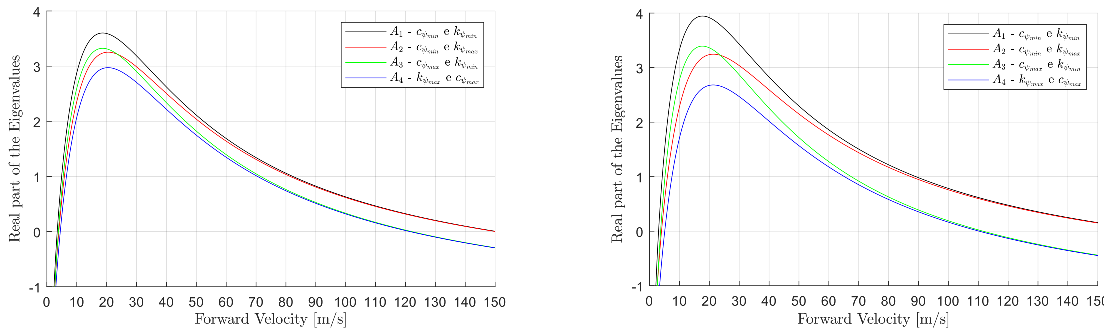

(a) $\delta_0 = 10\%$. (b) $\delta_0 = 20\%$.

Figure 5. Effect of structural uncertainties on shimmy linear boundaries.

The increase of the uncertain parameter make the system more unstable, because the parameters variation covers more values, both higher and lower for the torsional stiffness k_ψ and the torsional damping of the structure c_ψ. As it is possible to notice in both eigenvalues curves, the matrix $\mathbf{A}_1$ is is the point of greatest danger, which has the most real part of the complex eigenvalues. This is mainly because at this point, the combination of values for k_ψ and c_ψ are the least possible, allowing vibrations to propagate. Furthermore, when analyzing the Eq. (1), it is noticed that the places in which the k_ψ and c_ψ coefficients are located significantly influence the oscillations caused in the landing gear due to multiplying the torsional motion and velocity. Thus, the velocity V for each uncertain value was based on the point of greatest intensity in the shimmy effect for the matrix $\mathbf{A}_1$.

4.2 Control of shimmy instabilities

Using the methodology described in Section 3, the state feedback controller gains are obtained by solving the convex optimization problem of Eqs. (11). It is used the Matlab LMI toolbox considering $\mathbf{Q} = 0.001\mathbf{I}_{3\times3}$, $\mathbf{R} = 1$ and decay rate of $\gamma = 0.01$. These values were defined arbitrarily and the controllers are designed at the forward speed when the worst condition of instability is found. The controller's gains for 10% and 20% uncertainty are given by:

$$\mathbf{K}_{10\%} = \begin{bmatrix} -0.62520 & -0.04397 & 1.28826 \end{bmatrix}, \qquad \mathbf{K}_{20\%} = \begin{bmatrix} -0.99635 & -0.05152 & 1.46817 \end{bmatrix} \tag{12}$$

Based on these control gains, an eigenvalue analysis of the controlled shimmy system is carried out and depicted in Figure 6(a,b), respectively for 10% and 20% levels of uncertainty. Based on these results, it is verified the complete asymptotic stabilization of the system (i.e., for all shimmy boundary) with the implemented control strategy for the two uncertain scenarios, which can be confirmed by negative values of real parts eigenvalues.

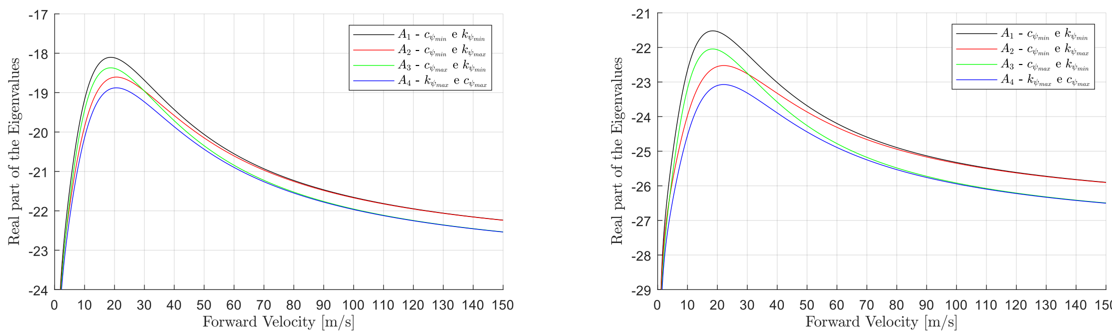

(a) $\delta_0 = 10\%$ (b) $\delta_0 = 20\%$.

Figure 6. Eigenvalues Curves for the Controlled System.

Figures 7 and 8 compares the uncontrolled and controlled time histories and phase portraits of the system, respectively. The four sub-systems are analyzed for 10% of uncertainty. Based on these results, it is verified the asymptotic stabilization of the LG for all vertices of the polytopic system.

Similarly, Figures 9 and 10 show the uncontrolled and controlled time histories and phase portraits of the LG, respectively, considering 20% of uncertainty. From these results, the asymptotic stabilization of the system it is observed for all vertices of the polytopic system.

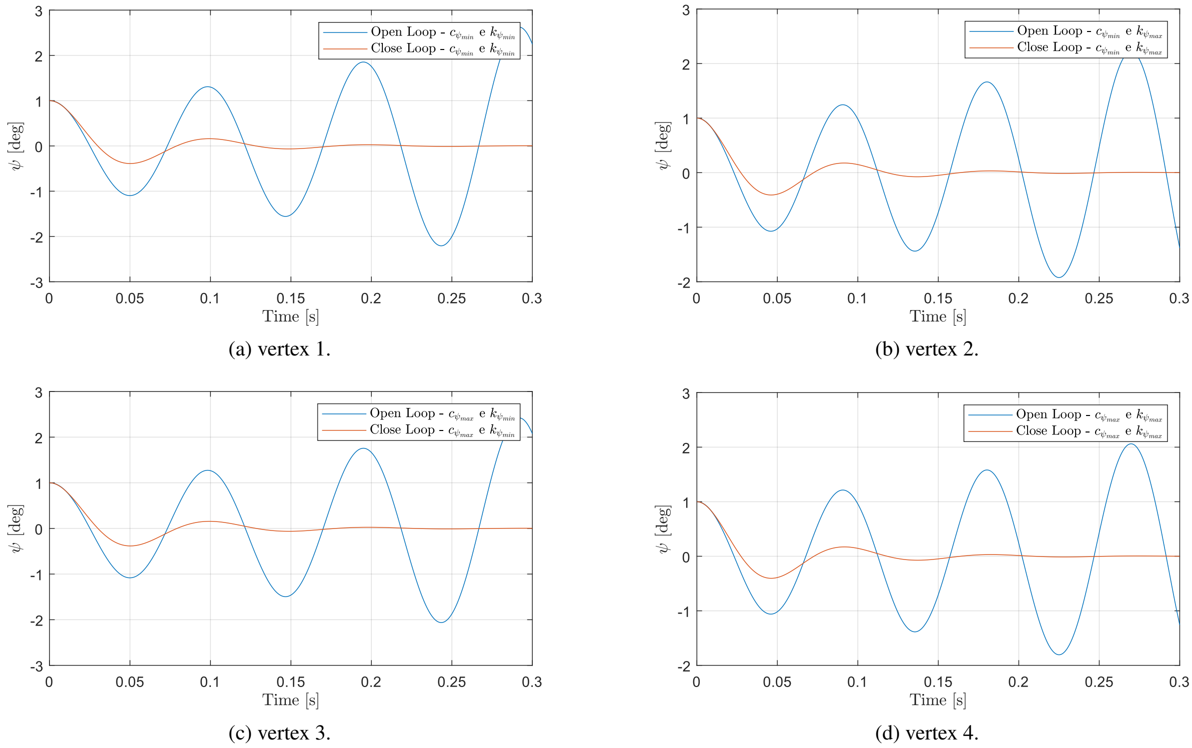

Figure 7. Comparison of the controlled and uncontrolled LG's torsional motion considering $\delta = 10\%$.

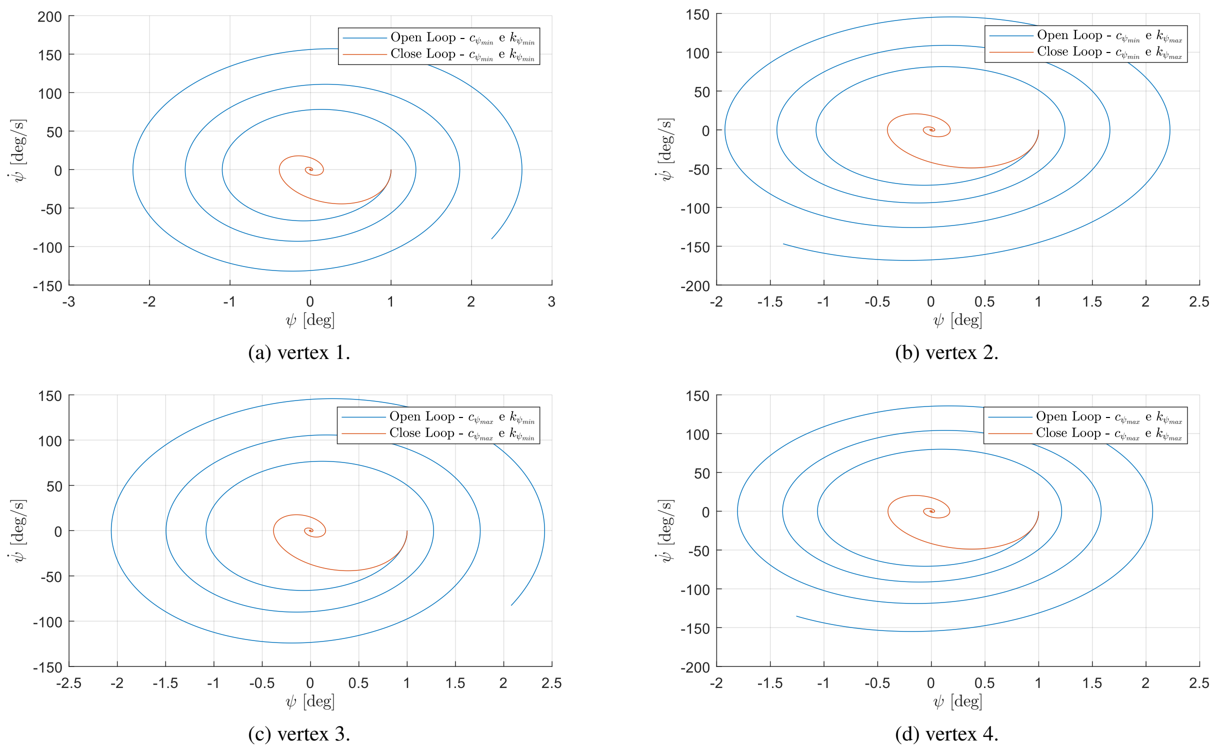

Figure 8. Comparison of the controlled and uncontrolled LG's phase portrait considering $\delta = 10\%$.

5. CONCLUSION

In the present paper, an alternative approach to design a robust controller to suppress the effect of linear shimmy phenomenon in the LG's structure has been proposed, in which the feedback controller gains were found using the solution of the convex optimization problem with LDQ performance index.

The classic model for the torsional shimmy was employed with the addition of a control moment. Structural uncer-

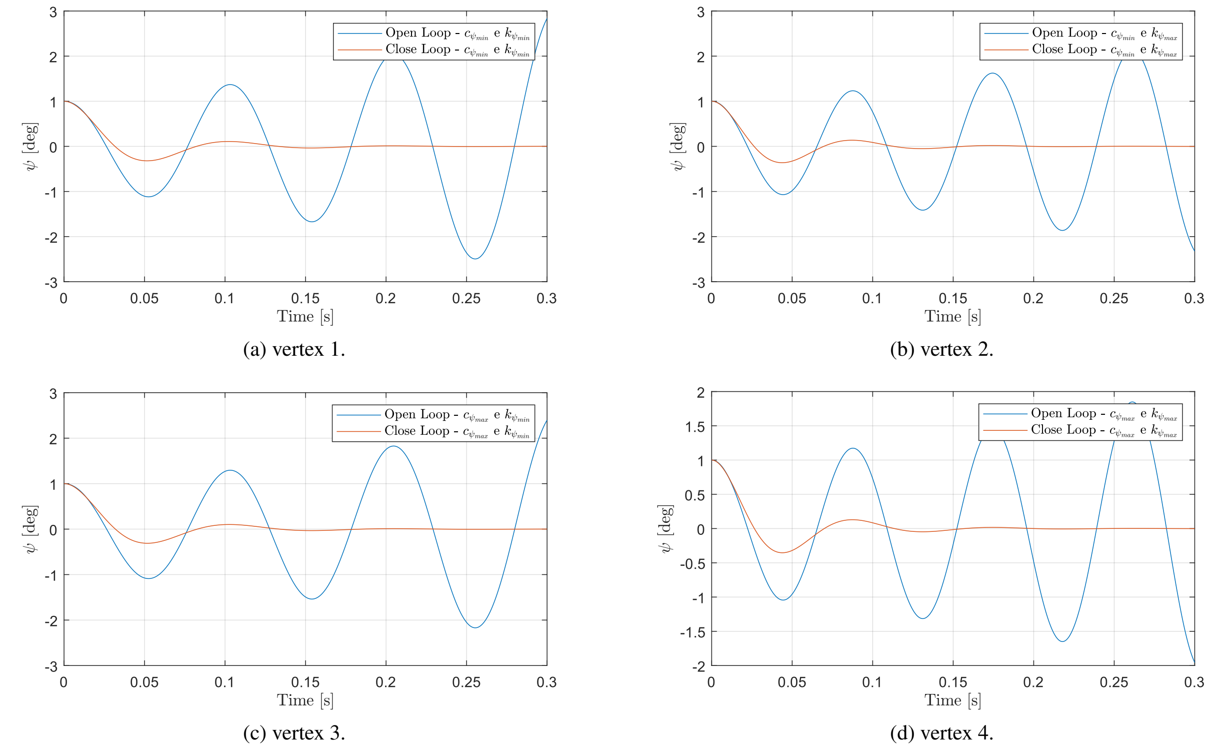

(a) vertex 1. (b) vertex 2. (c) vertex 3. (d) vertex 4.

Figure 9. Comparison of the controlled and uncontrolled LG's torsional motion considering $\delta = 20\%$.

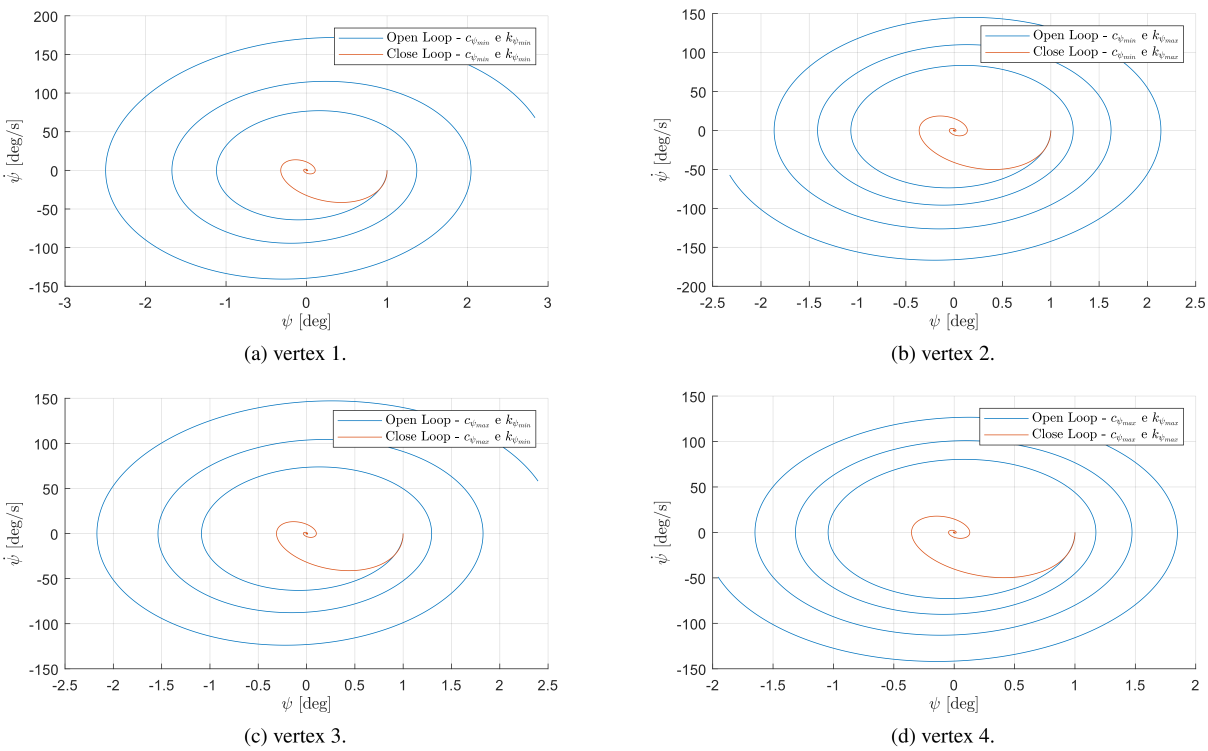

(a) vertex 1. (b) vertex 2. (c) vertex 3. (d) vertex 4.

Figure 10. Comparison of the controlled and uncontrolled LG's phase portrait considering $\delta = 20\%$.

tainties were modeled using the convex polytopic hull to represent the area that the controller should be designed to assure the system stability with LG's structural stiffness (k_ψ) and damping (c_ψ) as the parametric uncertainties. The LMI formulation has been defined with the Lyapunov stability theory and modified to present the Lyapunov matrix and the state feedback gain when the system is solved.

A numerical simulation for the linear shimmy was presented, in which, first, the open loop system was analyzed to locate the worst instability condition in the LG's structure. Then, the close loop system was considered and the controller gains for 10% and 20% uncertainty were computed using the Matlab LMI toolbox with arbitrary values for **Q**, **R** and γ to solve the LMIs system. Finally, the effectiveness of the controller was verified by comparing the controlled and uncontrolled torsional motion and phase portrait of the landing gear.

The results demonstrate that the proposed LMI-based robust controller approach can be used as an active control to suppress the shimmy instabilities, asymptotically stabilizing the aircraft landing operational envelope in the presence of model's uncertainties.

6. ACKNOWLEDGEMENTS

The authors acknowledge the financial support for this work from the São Paulo Research Foundation (FAPESP grants #2020/15787-0 and #2019/05410-9) and the National Council for Scientific and Technological Development (CNPq grant #306824/2019-1).

7. REFERENCES

da Silva, J.A.I., Bueno, D.D. and de Abreu, G., 2019. "On the controllers' design to stabilize ground resonance helicopter". *Journal of Vibration and Control*, Vol. 25, No. 23-24, pp. 2894–2909. doi:10.1177/1077546319873797.

Esmailzadeh, E. and Farzaneh, K., 1999. "Shimmy vibration analysis of aircraft landing gears". *Journal of Vibration and Control*, Vol. 5, No. 1, pp. 45–56.

Laporte, D.J., Lopes, V. and Bueno, D.D., 2020. "An approach to reduce vibration and avoid shimmy on landing gears based on an adapted eigenstructure assignment theory". *Meccanica*, Vol. 55, No. 1, pp. 7–17.

Li, Y., Howcroft, C., Neild, S.A. and Jiang, J.Z., 2017. "Using continuation analysis to identify shimmy-suppression devices for an aircraft main landing gear". *Journal of Sound and Vibration*, Vol. 408, pp. 234 – 251.

Olalla, C., Leyva, R., Aroudi, A.E. and Queinnec, I., 2009. "Robust lqr control for pwm converters: An lmi approach". pp. 2548–2558.

Orlando, C., 2020. "Nose landing gear simple adaptive shimmy suppression system". *Journal of Guidance, Control, and Dynamics*, Vol. 0, No. 0, pp. 1–15.

Orlando, C. and Alaimo, A., 2017. "A robust active control system for shimmy damping in the presence of free play and uncertainties". *Mechanical Systems and Signal Processing*, Vol. 84, pp. 551 – 569.

Rahmani, M. and Behdinan, K., 2019a. "Investigation on the effect of coulomb friction on nose landing gear shimmy". *Journal of Vibration and Control*, Vol. 25, No. 2, pp. 255–272.

Rahmani, M. and Behdinan, K., 2019b. "On the effectiveness of shimmy dampers in stabilizing nose landing gears". *Aerospace Science and Technology*, Vol. 91, pp. 272 – 286.

Rahmani, M. and Behdinan, K., 2019c. "Parametric study of a novel nose landing gear shimmy damper concept". *Journal of Sound and Vibration*, Vol. 457, pp. 299 – 313.

Somieski, G., 1997. "Shimmy analysis of a simple aircraft nose landing gear model using different mathematical methods". *Aerospace Science and Technology*, Vol. 1, No. 8, pp. 545 – 555.

Thota, P., Krauskopf, B. and Lowenberg, M., 2010. "Bifurcation analysis of nose-landing-gear shimmy with lateral and longitudinal bending". *Journal of Aircraft*, Vol. 47, No. 1, pp. 87–95.

Tourajizadeh, H. and Zare, S., 2016. "Robust and optimal control of shimmy vibration in aircraft nose landing gear". *Aerospace Science and Technology*, Vol. 50, pp. 1 – 14.

8. RESPONSIBILITY NOTICE

The authors are solely responsible for the printed material included in this paper.